

## EFFECTS OF POLYCRYSTALLINE DIAMOND TOOL RAKE ANGLE ON TURNING PROCESS OF HIGH SILICON ALUMINUM ALLOY

Guangfeng SHI<sup>1</sup>, Hua ZHANG<sup>2</sup>

*High-silicon aluminum alloy has been widely used in cylinder engine parts, but the rise of silicon content of the alloy in the same time also brings some difficulties to the cutting process. In this paper, the effects of rake angle of polycrystalline diamond (abbreviating PCD) tools on the cutting force, the tool-chip interface stress, the cutting temperature and the tool wear in the cutting process of the high-silicon aluminum alloy are simulated and analyzed by the finite element simulation software DEFORM-2D. The results show that a negative rake angle of the tool may be a good choice to get a balance between the tool wear and the cutting quality, which is a new try for the common tool usage with positive rake angle.*

**Keywords:** High silicon aluminum alloy; Cutting force and temperature; Stress; Wear; Simulation analysis

### 1. Introduction

With the automotive industry lightweight, energy-saving goals put forward, aluminum alloy engine instead of the original cast iron engine has become a trend [1]. High-silicon aluminum alloy which has small thermal expansion coefficient, low density and good wear resistance, is widely used in the field of engine manufacturing [2]. However, the machining performance of high-silicon aluminium alloy is poor, and then often causes tool wear and other serious phenomenon [3]. It is known that the continuance of compressive and shear deformation sequence at the chip incipient stage governs the high-pressure phase transformation (HPPT) as a function of rake angle and tool wear [4]. Furthermore, the heat generation during metal cutting processes affects materials properties and the tool wear [5]. And the relationship among the tool rake angle, the stress, the workpiece temperature and the tool wear can be optimized to get an

<sup>1</sup>School of Mechanical and Electrical Engineering, Changchun University of Science and Technology, Changchun, 130022, China, Email: shiguangfeng@cust.edu.cn

<sup>2</sup> School of Mechanical and Electrical Engineering, Changchun University of Science and Technology, Changchun, 130022, China, Email:15947994390@139.com

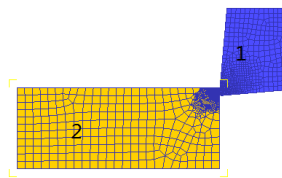
ideal cutting quality efficiently [6]. However, at present, the research on the influence of PCD tool rake angle on the thermal coupling in high-silicon aluminum alloy turning process has not been reported yet.

Based on the finite element simulation in DEFORM-2D [7], the relationship between the thermal coupling and the tool wear during turning the high-silicon aluminum alloy are studied by changing the rake angle of PCD tool, which can guide the tool design reasonably and improve the cutting quality of the workpiece.

## 2. Finite element model establishment

Though the chip deformation is three-dimensional in space during actual machining process, But the orthogonal cutting model is set up in DEFORM-2D in this paper to reveal the cutting mechanism conveniently because of the complexity of the cutting process in a three-dimensional state based on the following five assumptions: (1) The cutting width is at least five times bigger than the cutting depth. (2) The PCD tool is rigid with only a movement along the cutting direction. (3) The chip is produced continuously during the cutting process. (4) Ignoring the metallurgical structure and other chemical changes during metal processing due to temperature changes. (5) The material is isotropic.

Because metal cutting is a large deformation and high strain rate process, the quadrilateral element distortion is prone to produce during the simulation process. DEFORM-2D will automatically refine the element in the tool-workpiece interface and continuously re-divide the elements during the entire cutting simulation to avoid the large element deformation and improve convergence. Finally, the orthogonal simulation model is set up as shown in Fig.1.



1-tool, 2-part  
Fig.1. The finite element model

Al-20%Si high-silicon aluminum alloy is selected as the workpiece material whose chemical composition is shown in Table 1, and the material

mechanics parameters are density 2.78g/cm<sup>3</sup>, elastic Modulus 96000MPa, Yield strength 400MPa. In order to save the computing time, the workpiece geometry and process parameters of the simulation model are set as follows, length 2.5 mm, width 1 mm, cutting speed 2500mm/s, cutting depth 0.1mm, feed rate 0.1mm/r, ambient temperature 20 °C, shear friction coefficient 0.1, and heat transfer coefficient 70 N/sec/mm/C. The tool material is made of polycrystalline diamond (PCD), whose rake angle is chosen for 5 °, 0 °, -5 °, -10 °, -15 °, -20 °, -25 °, and -30 ° respectively. And the cutting edge radius of the tool is 0.02mm. The displacement method is used to simulate the cutting movement of the PCD tool.

Table 1.

Al-20% Si chemical composition

alloy composition	Si	Fe	Ni	Cu	Mn	Mg	Al
Content [%]	20	5	2	3	2	1	the remaining

The yield criterion is the Von Mises yield criterion [8], expressed as principal stress Eq.1,

$$(\sigma_1 - \sigma_2)^2 + (\sigma_2 - \sigma_3)^2 + (\sigma_3 - \sigma_1)^2 = 2\sigma_s^2 \quad (1)$$

where  $\sigma_s$  is the yield strength of the workpiece material. The non-dimensional Normalized Cockcroft & Latham fracture criterion is used for the finite element simulation. The fracture Eq.2 is

$$\int_0^{\bar{\varepsilon}_f} \frac{\sigma^*}{\bar{\sigma}} d \bar{\varepsilon} = C. \quad (2)$$

Where  $\sigma^*$  is the critical failure stress of the material;  $\bar{\sigma}$  is the true equivalent stress;  $\bar{\varepsilon}_f$  is the strain at the fracture of the material;  $\bar{\varepsilon}$  is the true equivalent strain; C is the fracture damage factor. Usui model is adaptive for continuous cutting conditions to calculate the tool wear [9], where the parameters are chosen for a = 1e-5 and b = 1000 empirically.

### 3. Simulation results analysis

*3.1 Effect of tool rake angle on the cutting force.* Cutting force is one of the main physical phenomena in the cutting process, which directly affects the cutting heat generation, the tool wear, and the machined surface quality. After the finite element model is computed, results can be analyzed by the post processor in Deform-2D. Fig.2 shows the cutting force curve along the x-direction (main

cutting force) when the tool rake angle is  $5^\circ$ . As the tool initial cutting, the material plastic deformation increases with the further increase of the tool cutting length, and the friction between tool-chip and tool-workpiece increases simultaneously. After forming a stable chip, the contact length between the tool and chip is almost unchanged. Then the chip continues to flow, and the cutting force tends to be stable, so the curve first increases quickly then declines a little and eventually keeps a steady trend. The fluctuation of cutting force in the steady state may be caused by the intermittent breaking of the workpiece material. It may also be due to the non-uniform distribution of the silicon particles inside the aluminum alloy.

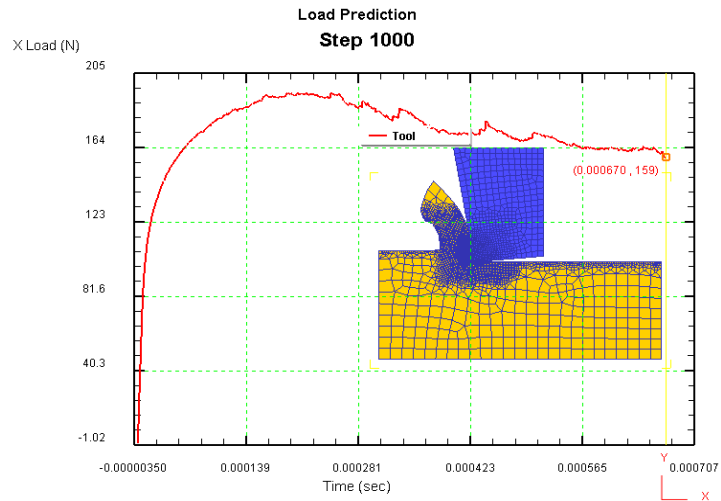


Fig.2. The simulated cutting force

Fig.3 and Fig.4 show the X,Y direction (thrust force) cutting forces for different tool rake angles. Compared with Fig.3 and Fig.4, it can be seen that the cutting forces of both x, y directions increase as the rake angle decreases from  $5^\circ$  to  $-30^\circ$ , but the variation of cutting force in y-direction is obviously larger than that in x-direction. This is because the rake angle plays a leading role in the extrusion process of the workpiece material with the tool rake angle increasing to negative values [10]. At the same time, the shear effect is weakened, while the radial force increases more. A strange phenomenon both in the Fig. 3 and Fig. 4 is that the output curves of the two cutting forces are very close to each other when the rake angle is  $-15^\circ$  and  $-20^\circ$ . What can account for this phenomenon is that there exists metal thermal soften effect in the cutting process when the tool reaches the angles in a range from  $-15^\circ$  to  $-20^\circ$ . The higher the deformation rate,

the more intensive the material dissipation, which consequently increases the temperature and facilitates the thermal softening then the hardness of the Al-20% Si high-silicon aluminum alloy decreases, so the material deformation costs a relatively small force.

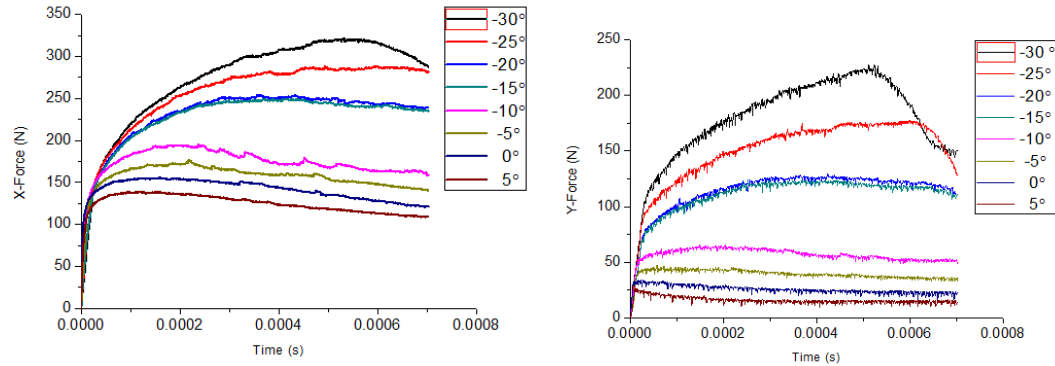


Fig.3. X-direction cutting force

Fig.4. Y-direction cutting force

In addition, it can be seen from Fig. 4 that unlike the common aluminum alloys such as 6061 and 7075, the cutting force curve of this type alloy in the y-direction is not smooth, there are countless small convex peaks during the entire cutting process, because with the increase of silicon content, the amount of primary crystal silicon increases, the hard particles formed uniformly distributes in the matrix of the high-silicon aluminum. On the one hand, hard points on the cutter with a mechanical scratch effect, on the other hand the workpiece hard grain boundaries at the hard point of the workpiece material can improve its strength and hardness, resulting in the development of the thrust force, so the force curve of y direction shows a tendency to many peaks.

*3.2 Effect of the tool rake angle on the interface stress.* The stress at the tool-workpiece contact area obtained by the point-tracking method in Deform-2D changes during the cutting process [11], as shown in Fig.5. The result different from the conclusion of Cheng Lin at Hefei University of Technology [12] is that the maximum equivalent stress always appears at the blunted edge of the cutting tip during the entire cutting process. With the cutting process continuing, the maximum equivalent stress shows a decline trend compared to its initial stage, and then the final state tends to be stable. The stress and change trend within the tool-chip contact length for different tool rake angles are shown in Fig. 6. The stress at each contact point increases as the rake angle increases towards the

negative direction, but the output stress curves at the stable state are also approximately coincident when the tool rake angle is  $-15^\circ$  and  $-20^\circ$  due to metal soften effect.

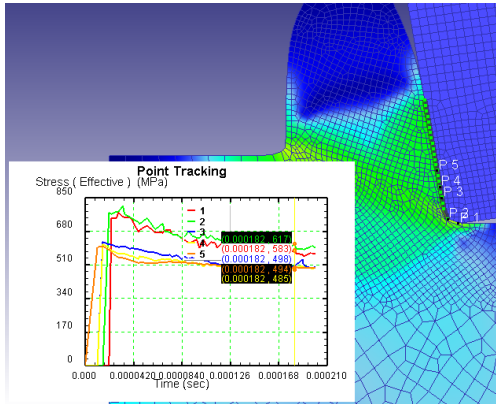


Fig.5The contact point stress

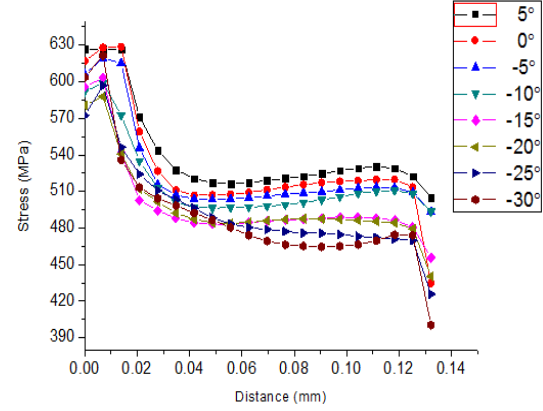


Fig.6The workpiece stress

*3.3 Effect of the tool rake angle on the cutting temperature.* In the cutting process, the cutting heat mainly comes from the material plastic deformation in the chip shear zone and the friction between the tool-chip interface, which leads the temperatures of the tool and the workpiece to rise rapidly.

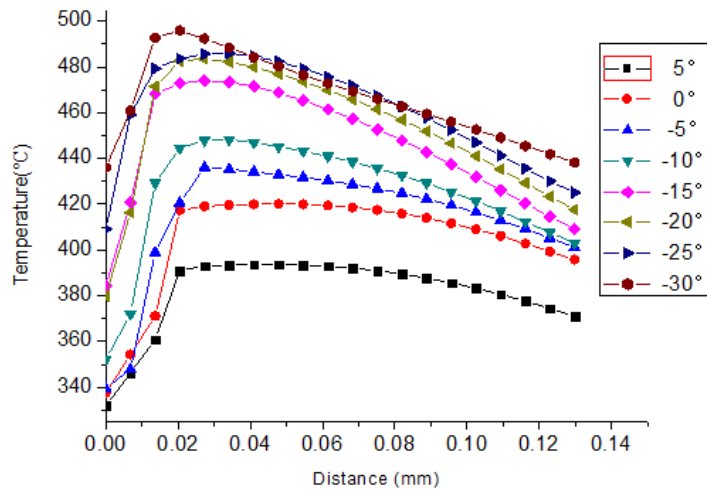
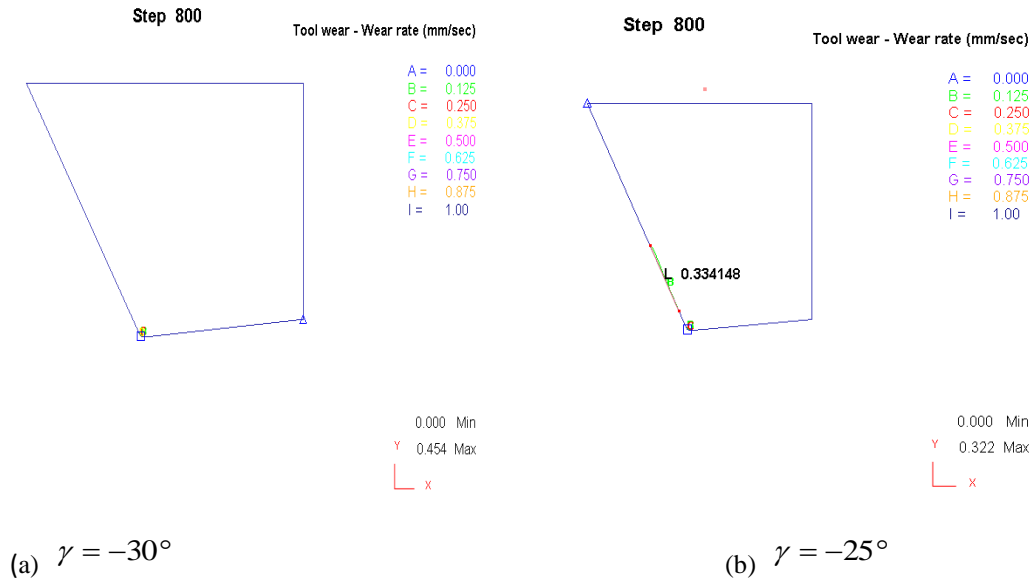


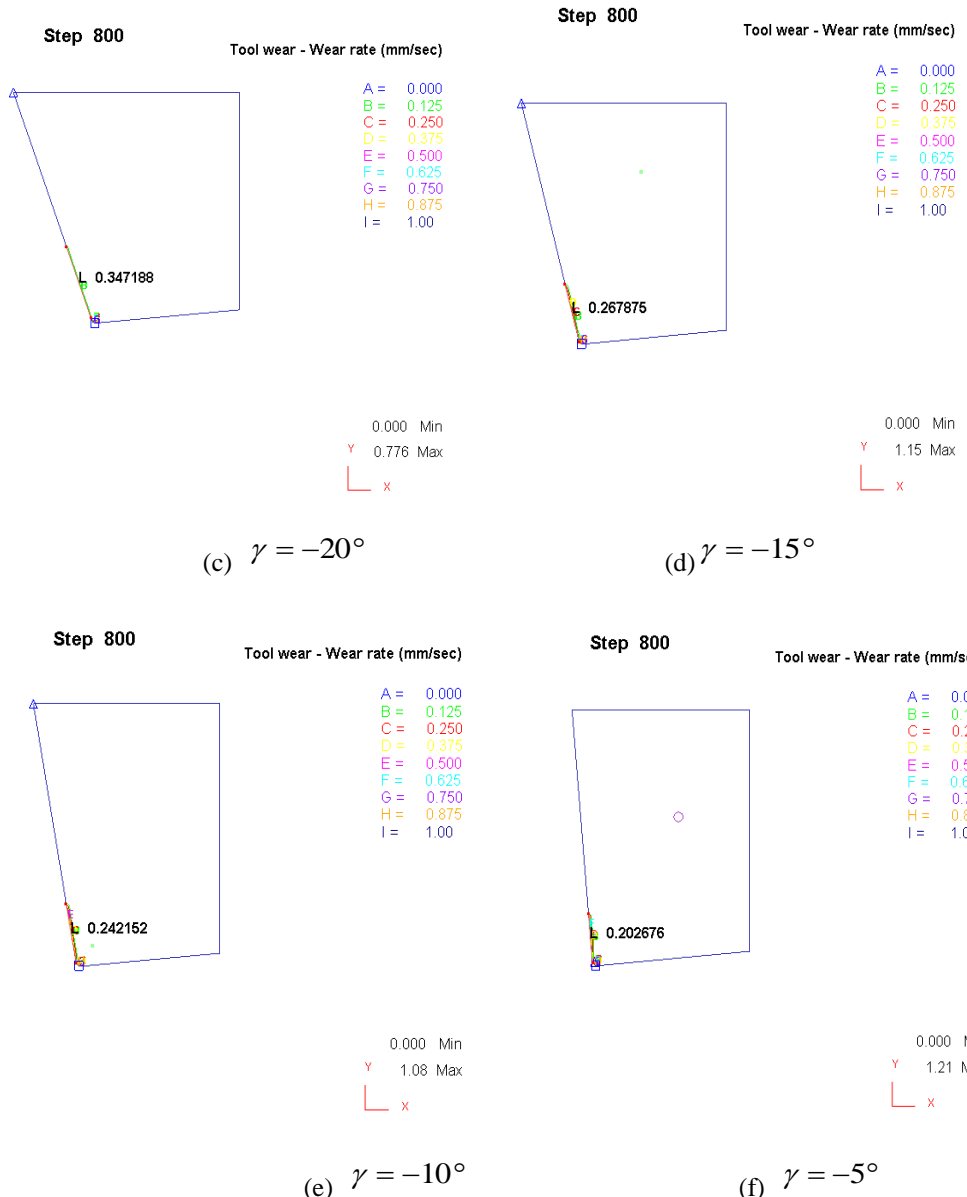
Fig.7Workpiece cutting temperature

It can be seen from Fig.7 that the maximum temperature has risen from  $390^\circ\text{C}$  to  $500^\circ\text{C}$  when the tool rake angle changed from  $5^\circ$  to  $-30^\circ$ , because the contact length of the tool-chip interface increases as the tool rake angle changes towards the negative values, which will result in the friction and temperature

increasing. The cutting action generates a large amount of heat, so the workpiece material appears a thermal softening effect which will lead the fracture and separation of the material to become relatively easy [13]. And the hardness of the workpiece material at the cutting area will decrease [14]. This reason also explains the aforementioned coincident phenomena of the stress curves when the tool rake angle is  $-15^\circ$  and  $-20^\circ$  as shown in Fig.3 and Fig.4.

*3.4 Effect of the rake angle on the worn length of the tool rake face.* When the tool rake angle is positive, the maximum temperature appears at the blunt cutting edge and the tool wear length is small [15], but the worn length of the tool does not show certain regularity in this paper when using negative rake angles. All the tool worn models of different rake angles are shown in Fig.8. The maximum temperature appears at the tool rake face with the corresponding tool worn length increase as the tool rake angle increases to negative, because the material in the cutting layer undergoes plastic deformation by the pressure of the tool rake face to separate from the workpiece during the cutting process. A large amount of heat is generated in the deformation process with the chip formed along the tool rake face to flow away, which will cause the tool wear. The tool worn lengths are listed in Table 2 by measuring it in DEFORM-2D.





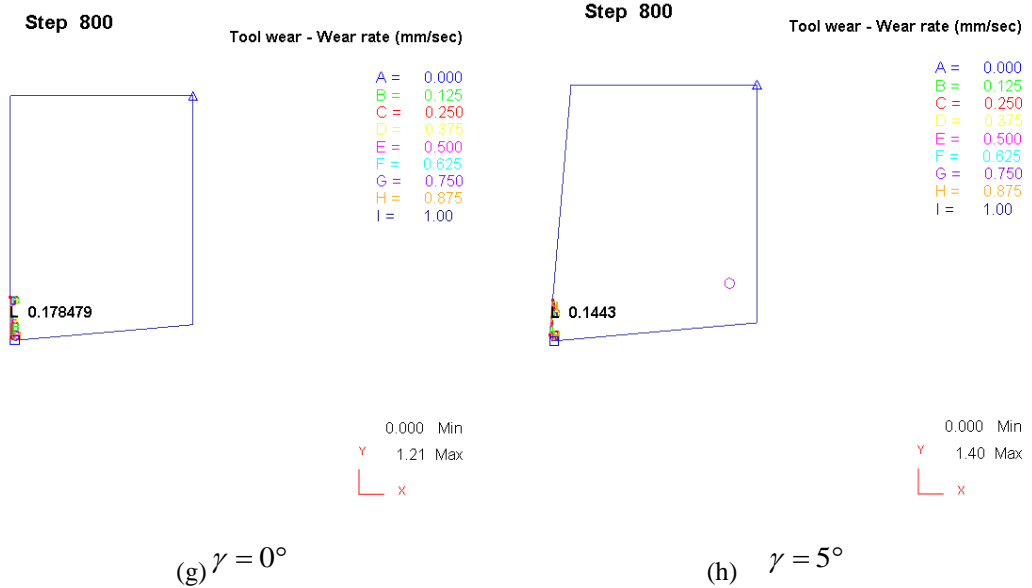


Fig.8 Tool wears length for different tool rake angles

Table 2 .

**Tool rake angle and the relationship between wear length**

Tool rake angle $\gamma$ [°]	5°	0°	-5°	-10°	-15°	-20°	-25°	-30°
Tool wear length L[mm]	0.144	0.178	0.203	0.242	0.268	0.347	0.334	0

Though there is a soften temperature to reduce the hardness of the workpiece material when the tool rake angle is  $-15^\circ$  and  $-20^\circ$ , the tool wear still increases because the rised temperature will get an adhesive wear based on Usui model for tool wear. But if cutting fluid is applied to this cutting condition to reduce the temperature and the adhesive wear, the soften effect will get a lighter tool wear for a equivalent tool-chip interface stress when the tool rake angle is  $-15^\circ$  and  $-20^\circ$  based on Usui model too. So, using a little negative rake angle ( $-15^\circ$  and  $-20^\circ$  in this paper) of the PCD tool can get an optimized result for cutting Al-20% Si high-silicon aluminum alloy. After all, the tool-tip interface stress is mainly decided by the negative rake face action of the PCD tool and the workpiece material. Whereas, the worn length of the tool rake face decreases after the rake angle reaches  $-25^\circ$ , even shows zero worn length at  $-30^\circ$ .

The former can be explained as the mechanical friction at the tool-chip interface plays a major role even though the temperature is still rising when the

tool rake angle reaches  $-25^\circ$ . The material flow rate decreases due to the negative tool angle resulted in a decrease at the worn length of the rake face, which shows nearly a zero worn length because of the existence of the stagnant zone where the material has a flow rate of zero and it exists throughout the cutting process with the large negative rake tool. The stagnation zone is characterized by the material flow rate equals zero or a strain rate of zero, shown as Fig.9 and Fig.10.

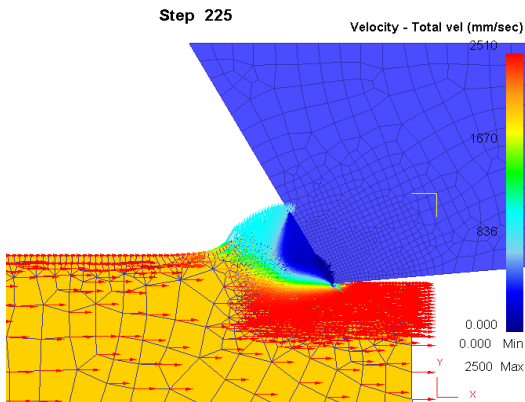


Fig.9 Stagnation zone(velocity=0)

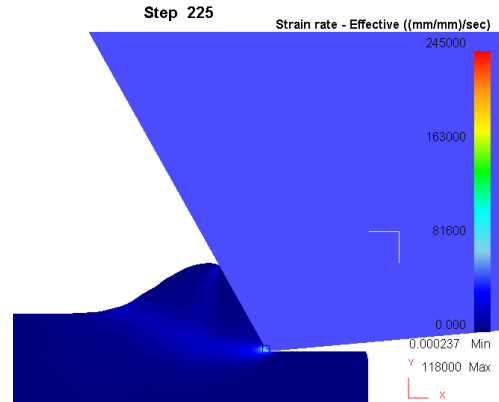
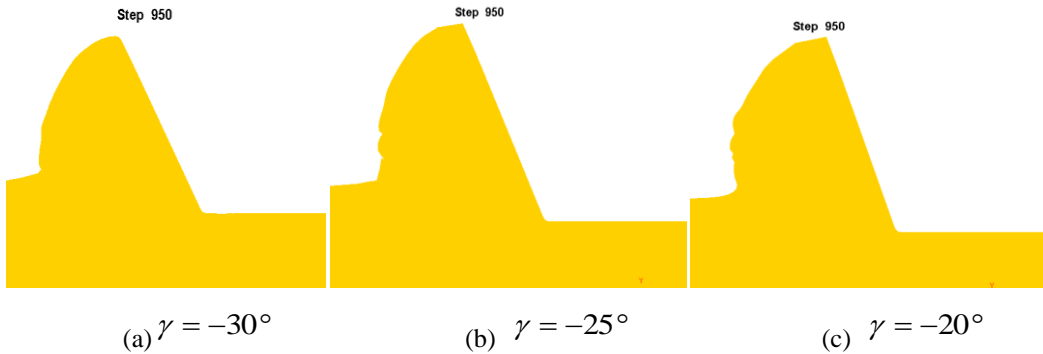


Fig.10 Stagnation zone (strain rate=0)

### 3.5 Relationship between the chip morphology and the tool rake angle.

When a high speed cutting is conducted at large plastic metal material, the tool rake angle will also have an effect on the chip morphology. It can be seen from Fig.11 that the more negative of the rake angle is, the more obvious of the wave chip morphology. From the viewpoint of metal shear deformation, although aluminum alloy material has a large plasticity, shear slip can be generated in the stress concentration zone in high-speed cutting at high strain rate and high-temperature cutting conditions. Under the action of extrusion and friction, part of the shear-slip band continues to slip upward and forward, resulting in wave-like corrugation chips.



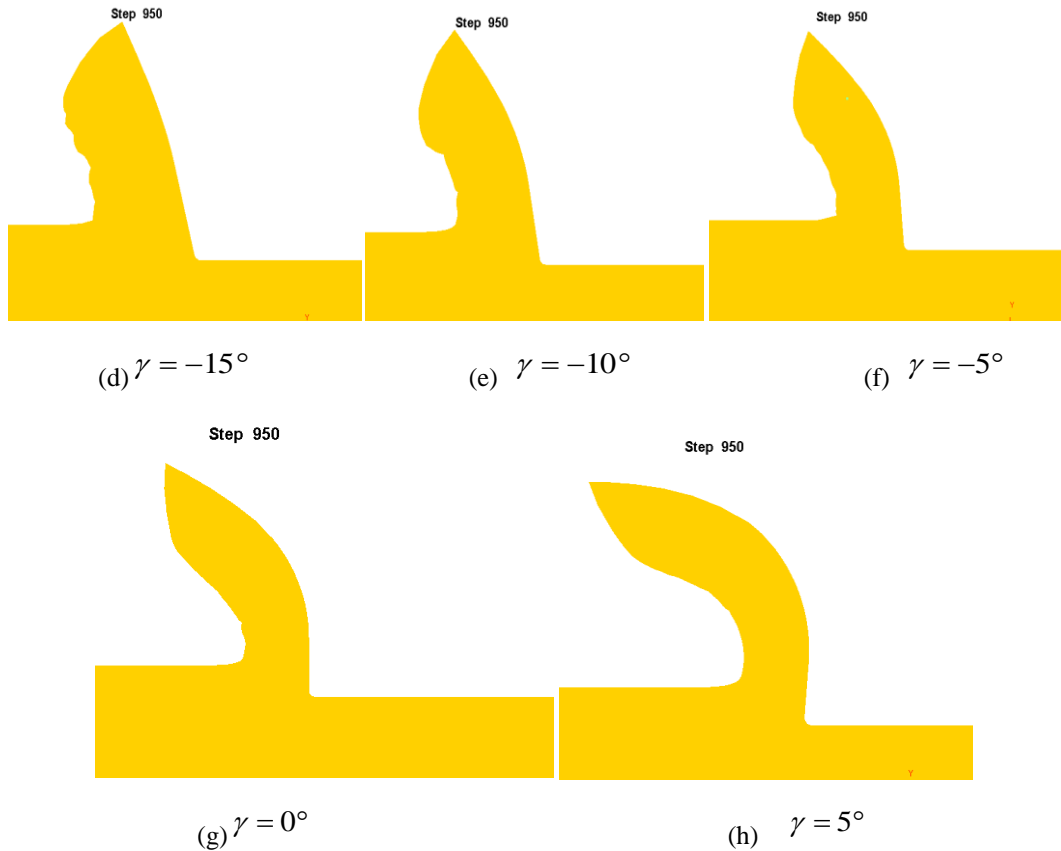


Fig.11 Chip morphology with different rake angles

#### 4. Conclusions

When Al-20% Si high-silicon aluminum alloy is cut by the PCD tool, the effect of the tool rake angle which changes from  $5^\circ$  to  $-30^\circ$  on the cutting force, the cutting temperature, the stress and the tool is studied by orthogonal cutting simulation in DEFORM-2D. It is known that the tool-tip interface stress at the stable cutting state are approximately coincident when the tool rake angle is  $-15^\circ$  and  $-20^\circ$ , which reveals the existence of a soften process at the workpiece material and it can be used for optimizing the tool rake angle to get an ideal cutting quality with accepted tool wear. Furthermore, a large negative rake angle maybe good for the use of tool when considering the worn length due to the existence of the workpiece stagnation zone in front of the tool rake face. Of course, the accurate conclusion should be further tested by the cutting experiment.

## Acknowledgement

This work is supported by the National natural science foundation of China (No.51405031, No.51575057).

## R E F E R E N C E S

- [1] *Cerit M, Coban M*, Temperature and thermal stress analyses of a ceramic-coated aluminum alloy piston used in a diesel engine, *J. International Journal of Thermal Sciences*, 77: 11-18. 2014.
- [2] *Shimizu Y, Spikes H A*, The Influence of Aluminium–Silicon Alloy on ZDDP Tribofilm Formation on the Counter-Surface, *J. Tribology Letters*, 65(4): 137. 2017.
- [3] *Soares R B, de Jesus A M P, Neto R J L, et al*, Comparison Between Cemented Carbide and PCD Tools on Machinability of a High Silicon Aluminum Alloy, *J. Journal of Materials Engineering and Performance*, 26(9): 4638-4657. 2017.
- [4] *Mir A, Luo X, Cheng K, et al*, Investigation of influence of tool rake angle in single point diamond turning of silicon, *J. The International Journal of Advanced Manufacturing Technology*, 1-13. 2017.
- [5] *Yaseen S J*, Theoretical study of temperature distribution and heat flux variation in turning process, *J. Al-Qadisiyah Journal for Engineering Sciences*, 5(3): 299-313. 2017.
- [6] *Daoud M, Chatelain J F, Bouzid A*, Effect of rake angle-based Johnson-Cook material constants on the prediction of residual stresses and temperatures induced in Al2024-T3 machining, *J. International Journal of Mechanical Sciences*, 122: 392-404. 2017.
- [7] *Pu Z, Umbrello D, Dillon O W, et al*, Finite element modeling of microstructural changes in dry and cryogenic machining of AZ31B magnesium alloy, *J. Journal of Manufacturing Processes*, 16(2): 335-343. 2014.
- [8] *Madenci E, Oterkus S*, Ordinary state-based peridynamics for plastic deformation according to von Mises yield criteria with isotropic hardening, *J. Journal of the Mechanics and Physics of Solids*, 86: 192-219. 2016.
- [9] *Lotfi M, Jahanbakhsh M, Farid A A*, Wear estimation of ceramic and coated carbide tools in turning of Inconel 625: 3D FE analysis, *J. Tribology International*, 99: 107-116. 2016.
- [10] *Deng W J, He Y T, Lin P, et al*, Investigation of the Effect of Rake Angle on Large Strain Extrusion Machining, *J. Materials and Manufacturing Processes*, 29(5): 621-626. 2014.
- [11] *Rajbanshi S K, Giri R N K, Gurung S, et al*, Machinability Study on Aluminium Metal Matrix Composite Using Finite Element Analysis, *J. Imperial Journal of Interdisciplinary Research*, 2(5). 2016.
- [12] *Cheng Lin*, Numerical simulation of stress field and temperature field in two-dimensional metal cutting, D. Hefei University of Technology, 2004
- [13] *Del Prete A, Franchi R, Mariano E*, Nickel Superalloy Components Surface Integrity Control through Numerical Optimization, C//Key Engineering Materials. Trans Tech Publications, 611: 1396-1403. 2014.
- [14] *Zhang W, He F, Wu T, et al*, 3D numerical simulation on thermal-stress distribution of hardened steels workpiece assembled with different hardness, *J. International Journal on Interactive Design and Manufacturing (IJIDeM)*, 11(3): 559-568. 2017.
- [15] *Singh A P, Singh E R B*, In metal turning effect of tool rake angles and lubricants on cutting tool life and surface finish: A Review. 2016.